Supporting Information for "Observation-based Trends of the Southern Ocean Carbon Sink"

R. Ritter[1], P. Landschützer[2,1], N. Gruber[1], A. R. Fay[3], Y. Iida[4], S. Jones[5,6], S. Nakaoka[7], G. -H. Park[8], P. Peylin[9], C. Rödenbeck[10], K. B. Rodgers[11], J. D. Shutler[12], and J. Zeng[7]

[1]Institute of Biogeochemistry and Pollutant Dynamics, ETH Zürich, Zürich, Switzerland

[2]Max Planck Institute for Meteorology, Hamburg, Germany

[3]Lamont-Doherty Earth Observatory, Columbia University, New York, USA

[4]Global Environment and Marine Department, Japan Meteorological Agency, Tokyo, Japan

[5]Geophysical Institute, University of Bergen, Bergen, Norway

[6]Bjerknes Centre for Climate Research, Bergen, Norway

Contents of this File

1. Text S1 to S2

2. Datasets S1 to S3

3. Figures S1 to S3

[7]National Institute for Environmental Studies, Tsukuba, Japan

[8]East Sea Research Institute, Korea Institute of Ocean Science and Technology, Uljin, Republic of Korea

[9]Laboratoire des Sciences du Climat et de l'Environnement (LSCE), Gif sur Yvette, France

[10]Max Planck Institute for Biogeochemistry, Jena, Germany

[11]Atmospheric and Oceanic Sciences Program, Princeton University, New Jersey, USA

[12]College of Life and Environmental Sciences, University of Exeter, United Kingdom

4. Table S1

S1. Observation-based pCO_2 Mapping Methods

We use a subset of 9 out of the 14 pCO_2 mapping products collected by the SOCOM project [*Rödenbeck et al.*, 2015]. The following 9 members of the SOCOM ensemble are retained for the analysis: ETH-SOMFFN, Jena-MLS, PU-MCMC, UEA-SI, AOML-EMP, CARBONES-NN, NIES-NN, CU-SCSE and JMA-MLR. Five ensemble members are products building on predictor-observation relationships, either by linear regression (AOML-EMP [*Park et al.*, 2010], JMA-MLR [*Iida et al.*, 2015]) or non-linear relationships derived from neural network approaches, i.e., those building on a feed-forward network (NIES-NN [*Zeng et al.*, 2014], CARBONES-NN (http://www.carbones.eu/wcmqs/)) or on a combination of both clustering and regression (ETH-SOMFFN [*Landschützer et al.*, 2016]). Other approaches include statistical data interpolation methods based on observed data correlation lengths (UEA-SI [*Jones et al.*, 2015]), a mixed-layer budget (Jena-MLS [*Rödenbeck et al.*, 2013]) and an empirical orthogonal function (EOF) analysis of an ensemble of process model simulations (CU-SCSE). Finally, the SOCOM ensemble further includes methods that rely on data-based regression and tuning of ocean forward models (PU-MCMC [*Majkut et al.*, 2014]). The complementary nature of this ensemble allows us to identify ΔpCO_2 trends independent of the chosen data-extrapolation or mapping method.

S2. Spatial Residuls

The spatial residuals of pCO_2 (pCO_2^{est} - $pCO_2^{SOCATv2}$) in µatm for the period from 1990 through 2009 are presented in Figure S3.

From a first point of view the spatial residuals with the SOCATv2 data of the most methods are randomly distributed (over- and underestimations are in balance). Anyhow most of the methods tend to overestimate the pCO_2 values around the SO shores (positive discrepancies in red).

To overcome deceptive visual conclusions with respect to the spatial randomness of the residuals in the SO basin, we further present the results from the quantitative residual assessment for tree different sectors. The spatial mean biases for the SOCATv2 are tabulated for following SO sub-sectors: the Pacific sector (160°E-60°W), the Atlantic sector (60°W-30°E) and the Indian sector (30°E-160°E) (Table S1).

Dataset S1. Trends calculated from the pCO_2 Mapping Methods

DatasetS1 of includes ΔpCO_2 (in μatm yr^{-1}) and air-sea CO_2 flux trends (in Pg C yr^{-1} decade^{-1}) calculated for the 9 participating mapping methods and their multi-model mean for the periods 1990-1999 and 2000-2010. The numbers correspond to panel (b) of Figure 1 in the main article.

Dataset S2. 1x1° multi-model mean ΔpCO_2 trend from 1990-1999

DatasetS2 contains the mean ΔpCO_2 trend (in μatm yr^{-1}) of the multi-model product for each 1x1° pixel from 1990-1999. The numbers correspond to panel (a) in Figure 3 of the main manuscript.

Dataset S3. 1x1° multi-model mean ΔpCO_2 trend from 2000-2009

DatasetS3 contains the mean ΔpCO_2 trend (in μatm yr^{-1}) of the multi-model product for each 1x1° pixel from 2000-2009. The numbers correspond to panel (b) in Figure 3 of the main manuscript.

References

Iida, Y., A. Kojima, Y. Takatani, T. Nakano, H. Sugimoto, T. Midorikawa, and M. Ishii, Trends in pCO_2 and sea-air CO_2 flux over the global open oceans for the last two decades, *Jornal of Oceanography*, *71*, 637–661, doi:10.1007/s10872-015-0306-4, 2015.

Jones, S. D., C. Le Quéré, C. Rödenbeck, A. C. Manning, and A. Olsen, A statistical gap-filling method to interpolate global monthly surface ocean carbon dioxide data, *Journal of Advances in Modeling Earth Systems*, *07*, 1942–2466, doi:10.1002/2014MS000416, 2015.

Landschützer, P., N. Gruber, and D. C. E. Bakker, Decadal variations and trends of the global ocean carbon sink, *Global Biogeochemical Cycles*, *30*, 1396–1417, doi:10.1002/2015GB005359, 2015GB005359, 2016.

Majkut, J. D., J. L. Sarmiento, and K. B. Rodgers, A growing oceanic carbon uptake: Results from an inversion study of surface pCO_2 data, *Global Biochemical Cycles*, *28*, 335–351, doi:10.1002/2013GB004585, 2014.

Park, G.-H., R. Wanninkhof, S. C. Doney, T. Takahashi, K. Lee, R. A. Feely, C. L. Sabine, J. Triñanes, and I. D. Lima, Variability of global net sea–air CO_2 fluxes over the last three decades using empirical relationships, *Tellus B*, *62*(5), 352–368, doi:10.1111/j.1600-0889.2010.00498.x, 2010.

Rödenbeck, C., R. Keeling, D. Bakker, N. Metzl, A. Olsen, C. Sabine, and M. Heimann, Global surface-ocean pCO_2 and sea-air CO_2 flux variability from an observation-driven ocean mixed-layer scheme, *Ocean Science*, *9*, 93–216, doi:10.5194/os-9-193-2013, 2013.

Rödenbeck, C., et al., Data-based estimates of the ocean carbon sink variability - first results of the Surface Ocean pCO_2 Mapping intercomparison (SOCOM), *Biogeosciences*, *12*(23), 7251–7278, doi:10.5194/bg-12-7251-2015, 2015.

Zeng, J., Y. Nojiri, P. Landschützer, M. Telszewski, and S. Nakaoka, A Global Surface Ocean fCO_2 Climatology Based on a Feed-Forward Neural Network, *Journal of Atmospheric and Oceanic Technology*, *31*(8), 1838–1849, doi:10.1175/JTECH-D-13-00137.1, 2014.

Table S1. SO spatial mean bias between the estimates and the SOCATv2 observations for the period from 1990 through 2009 for the three SO sub-sectors: Pacific sector (160°E-60°W), the Atlantic sector (60°W-30°E) and the Indian sector (30°E-160°E). Values between ±0.1 are considered as not significant (n.s.). All values are in µatm.

Mapping Method	Pacific Sector	Atalntic Sector	Indian Sector
ETH-SOMFFN	1.4	0.01	0.01
Jena-MLS	1.7	0.01	0.07
PU-MCMC	0.5	-0.03	0.01
UEA-SI	-0.3	-0.02	-0.05
AOML-EMP	2.0	0.12	n.s
CARBONES-NN	0.6	-0.04	-0.02
NIES-NN	1.4	0.02	0.12
CU-SCSE	2.2	0.03	0.03
JMA-MLR	0.4	0.03	-0.06

Figure S1. (a) Data density of the SOCATv2 database from 1990 through 1999 and (b) from 2000 through 2009 in number of gridpoints i.e. months with data. White areas are areas where no data exist.

Figure S2. Box-whiskers plots of the bias (residual) between the 9 gridded estimates and the SOCATv2 observations for five year temporal intervals from 1990 through 2009 averaged over the SO biomes (ice-weighted). The whiskers show the bias median (red line in each box), the 25^{th} and 75^{th} percentiles (blue box upper and bottom line, respectively), outliers (biases outside of the 95% confidence range, in red crosses). Values which lay outside the range between -50 and 50 µatm are directly placed on the borderlines.

Figure S3. SO spatial residuals of pCO_2 (pCO_2^{est} - $pCO_2^{SOCATv2}$) in µatm for the period from 1990 through 2009.

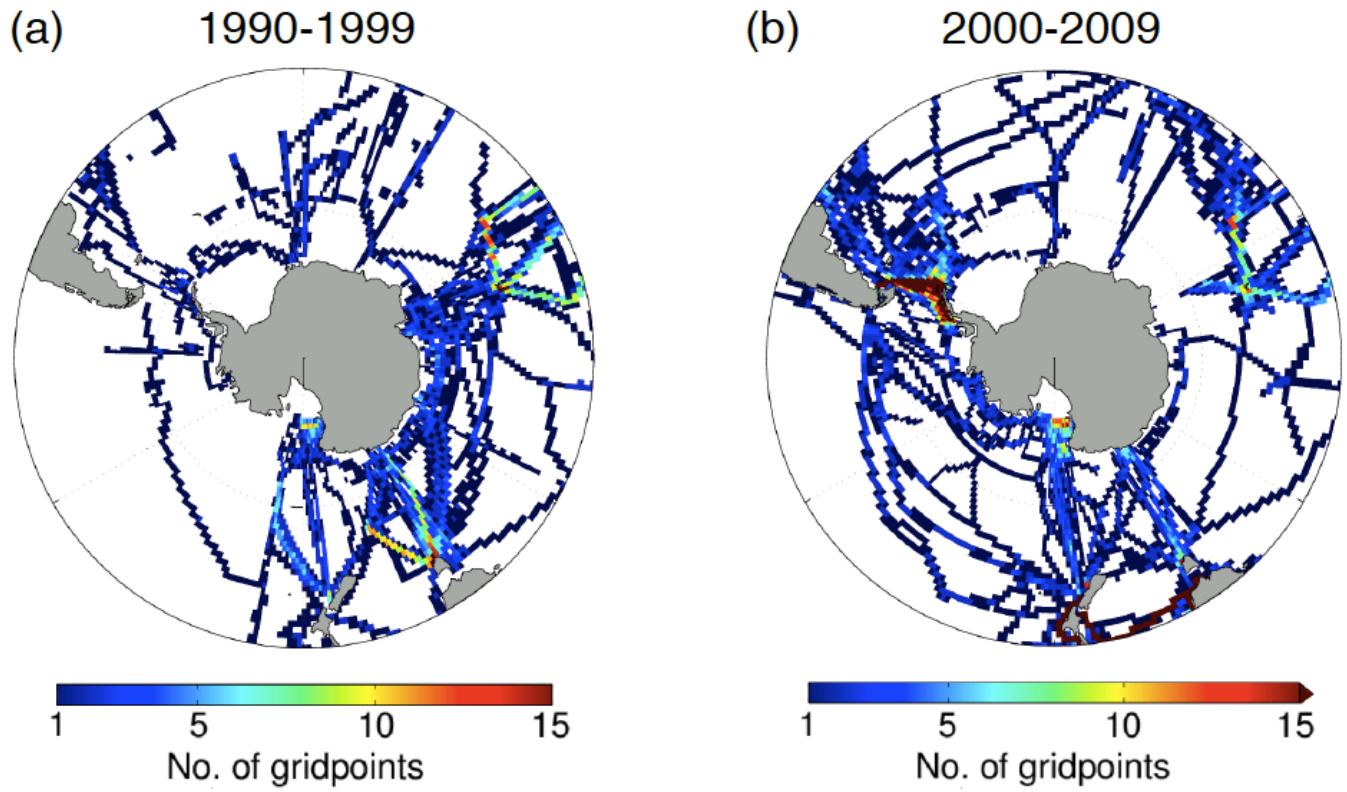
(a)
1990-1999
(b)
2000-2009
1
5
10
15
No. of gridpoints
1
5
10
15
No. of gridpoints

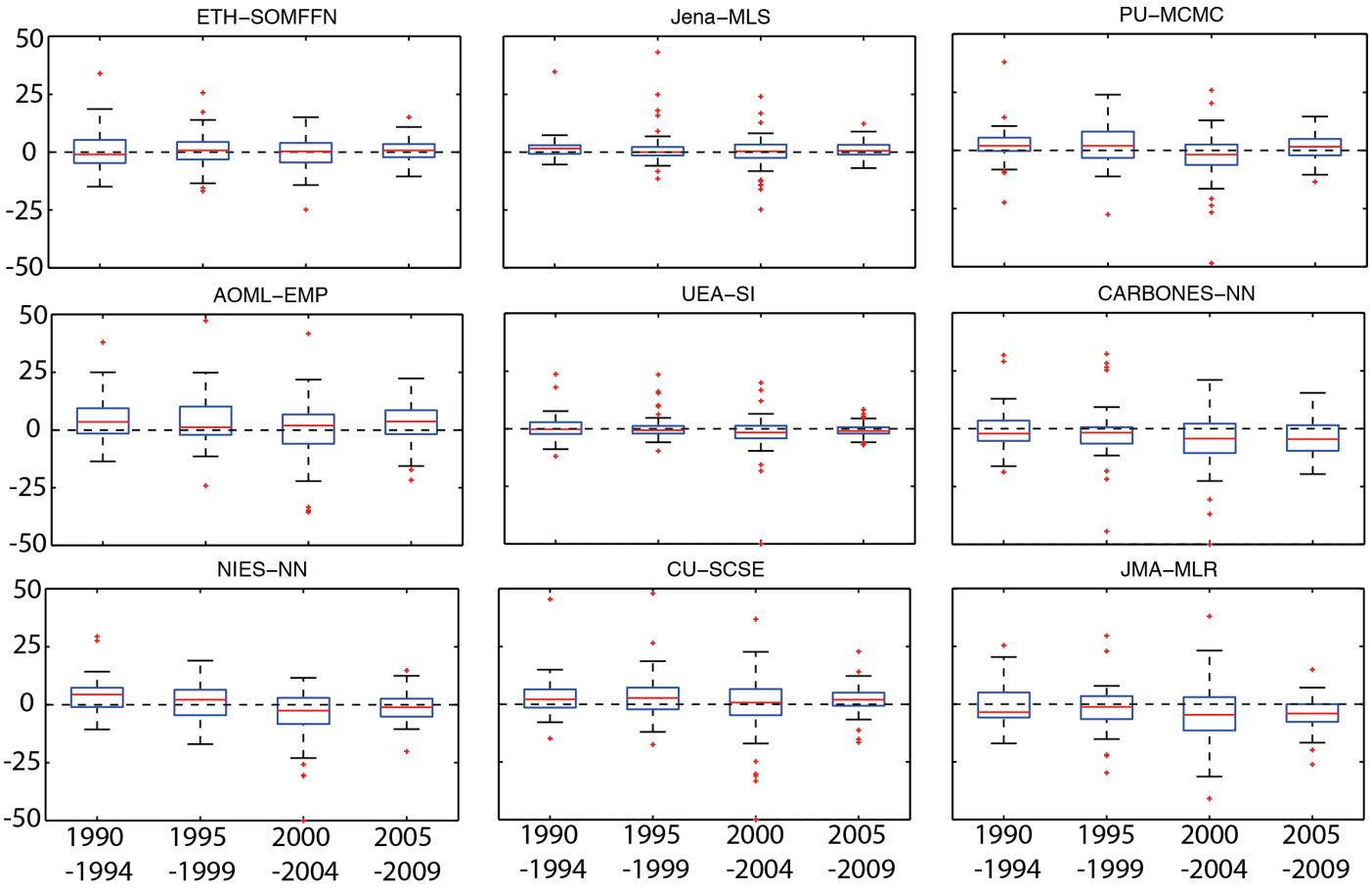
ETH–SOMFFN
Jena–MLS
PU–MCMC
AOML–EMP
UEA–SI
CARBONES–NN
NIES–NN
CU–SCSE
JMA–MLR
50
25
0
-25
-50
1990
-1994
1995
-1999
2000
-2004
2005
-2009

ETH-SOMFFN - SOCATv2

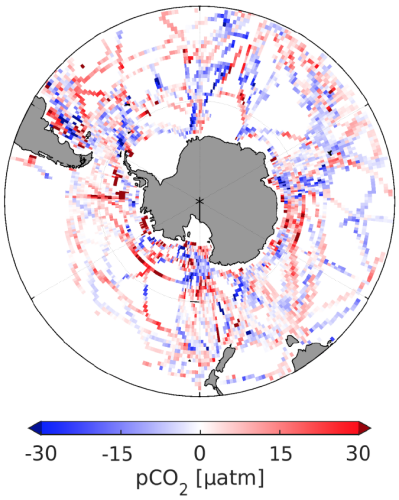

Jena-MLS - SCOATv2

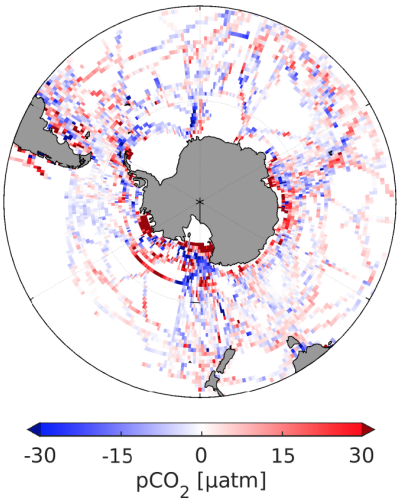

PU-MCMC - SOCATv2

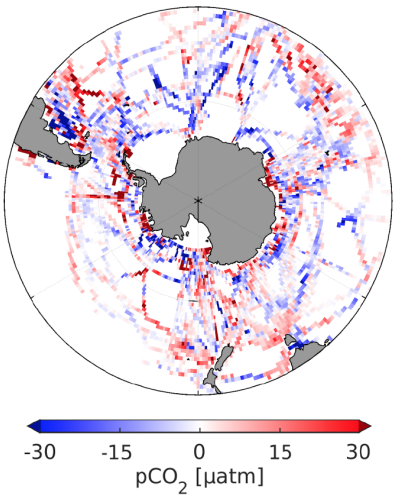

AOML-EMP - SOCATv2

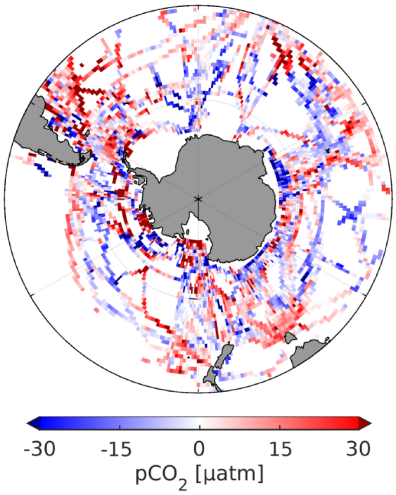

UEA-SI - SOCATv2

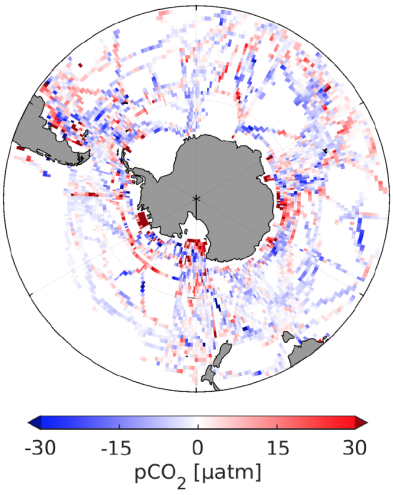

CARBONES-NN- SOCATv2

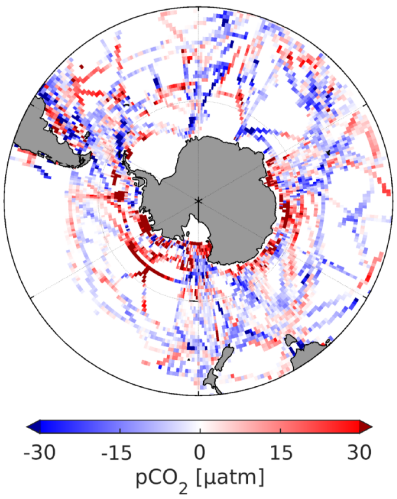

NIEAS-NN - SOCATv2

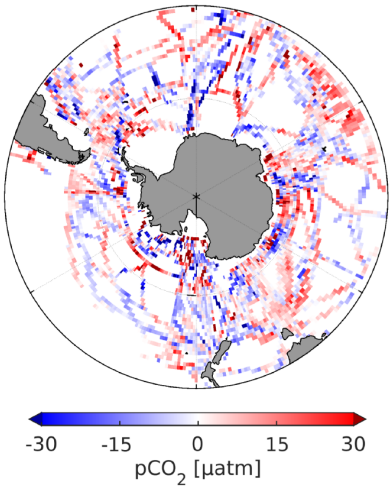

CU-SCSE - SOCATv2

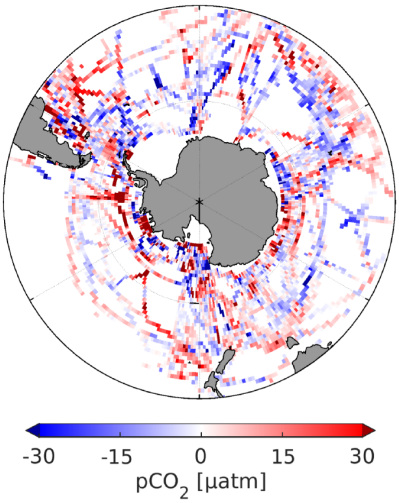

JMA-MLR - SOCATv2